Articles in PresS. J Appl Physiol (May 24, 2007). doi:10.1152/japplphysiol.00199.2007

Final Accepted Manuscript: JAP-00199-2007.R2

Flow-induced shear strain in intima of porcine coronary arteries

Wei Zhang[1], Yi Liu[1], and Ghassan S. Kassab[1,2,3]

[1]Department of Biomedical Engineering, [2]Surgery and [3]Cellular and Integrative Physiology, IUPUI, Indianapolis, IN 46202, USA

RUNNING HEAD: Flow-induced shear strain in intima

Address correspondence: G. S. Kassab, Department of Biomedical Engineering, IUPUI, 723 W. Michigan Street, Indianapolis, IN 46202 (e-mail: gkassab@iupui.edu).

Final Accepted Manuscript: JAP-00199-2007.R2

ABSTRACT

The *in vivo* circumferential strain has a small variation throughout the vascular system (aorta to arterioles). The axial strain has also been shown to be nearly the same as the circumferential strain under physiological loading. Since the endothelium is mechanically much softer than the media-adventitia in healthy arteries, the porcine intima was considered as a mechanically distinct layer from the media-adventitia in a two-layer computational model. Based on the simulation result, we hypothesize that the flow-induced shear strain in intima can be of similar value as the pressure-induced circumferential strain in healthy coronary arteries even though the shear stress is orders of magnitude smaller than the circumferential stress. The nearly isotropic deformation (circumferential, axial, and shear strains) may have important implications for mechanical homeostasis of endothelial cells, mechanotransduction, growth and remodeling of blood vessels.

KEYWORDS: Endothelium; stress; deformation; mechanotransduction

Final Accepted Manuscript: JAP-00199-2007.R2

INTRODUCTION

Blood vessels are subjected to mechanical loadings such as internal blood pressure, flow -induced shear, and tethering from surrounding tissues. It is believed that a mechanical homeostatic state exists in blood vessels (22). Although stress and strain may vary throughout the circulatory system, the variation is relatively small, particularly for the strain (12). A remodeling response is initiated when a change in the loading conditions (blood pressure, flow, surrounding tissue, etc.) perturbs the mechanical homeostasis. The response is an adaptation to restore the homeostatic state (22). The mechanical homeostasis can be described by the *uniform strain* hypothesis which states that the *in vivo* transmural circumferential strain is uniform in the vessel wall (13,37). This hypothesis can be extended for the mean wall strain measured in reference to the zero-stress state which has been found to be remarkably uniform in the coronary arterial tree and aorta (12). Zhang *et al*. (42) found that the circumferential and axial strains tend to be uniform and equal in the arterial wall under physiological loading.

An arterial wall is typically composed of three functional layers from inner to outer wall surfaces: intima, media, and adventitia. The intima comprises a single layer of endothelial cells and a basal lamina in normal vessels. The media consists mainly of smooth muscle cells, elastin and collagen fibrils. The adventitia contains mainly collagen fibers, ground substance, fibroblasts and fibrocytes. Since the intima is very thin and much more compliant than the media and the adventitia, its material property is generally ignored. Consequently, blood vessels are typically viewed either as a single layer of homogeneous material (3,5,19,32) or as a two-layer composite of intima-media and adventitia under normal conditions (16,26,27,34,39). It has been well accepted that endothelial cells (the major constituent of intima) are very sensitive to changes in flow-induced shear stress, and many biological activities are related to this shear loading

Final Accepted Manuscript: JAP-00199-2007.R2

(7,4,30,35,40,31,38,1). For instance, the diameter and thickness of the vessel wall are modulated by flow-induced shear stress, even though the shear stress is several orders of magnitude smaller than the circumferential wall stress. This raises the question of why blood vessels are so sensitive to such small loading. Our hypothesis is that shear strain can be substantial in endothelial cells despite the small shear stress. Our rationale is that the deformation of endothelium can be underestimated if the mechanical property of intima is not considered individually.

Most previous investigations on the mechanics of vessel wall have focused on the pressure-induced normal stress and strain. The shear strain, however, due to relatively small magnitude of flow-induced shear stress has not received significant attention. In this study, we will examine the shear deformation in arterial walls under physiological pressure and flow conditions. We will demonstrate that the flow-induced shear strain in the intima layer can be of the same magnitude as normal (circumferential and axial) strains caused by pressure and axial pre-stretch. This result may shed light on mechanotransductory mechanisms in blood vessels as well as arterial growth and remodeling modulated by the mechanical environment of endothelial cells.

Glossary

r	Radial coordinate, deformed
θ	Circumferential coordinate, deformed
z	Axial coordinate, deformed
w	Axial displacement of arterial wall
R	Radial coordinate, zero-stress
Θ	Circumferential coordinate, zero-stress

Z	Axial coordinate, zero-stress
Φ	Opening angle
χ	Defined as $\chi = \pi/(\pi-\Phi)$
H	Hydrostatic stress
P	Internal blood pressure
τ	Shear stress at inner surface
μ	Coefficient of viscosity
Q	Rate of flow
L	Length for which pressure drops ΔP
W	Strain energy function
C	Parameter in Fung strain energy (kPa)
b_α	Parameters in Fung strain energy ($\alpha = 1,\ldots,7$)
λ_m	Stretch ratios ($m = r, \theta, z$)
ξ_w	Defined as $\xi_w = dw/dR$
i, o	Subscripts, inner/outer surface
j, k	Subscript indexes ($j, k = r, \theta, z$)
δ_{jk}	Kronecker delta tensor
F_{jk}	Deformation gradient tensor
E_{jk}	Green strain tensor
σ_{jk}	Cauchy stress tensor

Final Accepted Manuscript: JAP-00199-2007.R2

MATERIALS AND METHODS

Mathematical Model

To make the problem analytically tractable, we consider an artery segment that is mechanically homogeneous, cylindrically orthotropic, and volumetrically incompressible in each respective layer. It is further assumed that the artery remains as a straight cylinder with uniform thickness along the axial direction in the loaded state (Fig. 1*A*). The zero-stress state is represented by an open sector as shown in Fig. 1*B*, wherein the opening angle Φ characterizes the circumferential residual strain (5) at the no-load state (i.e., a tube with zero pressure and shear). The deformed cross-section is schematically shown in Fig. 1*C*, where the axial (z) direction is pointing out of the r-θ plane. We employ a two-layer model in which the intima is considered different from the rest of the wall; i.e., the media-adventitia layer (Fig. 1*D*). This treatment differs from the classic intima-media and adventitia two-layer model (16,39), since the significance of intima layer is of interest in this work.

More specifically, we assume that the artery deforms uniformly in the axial direction and the deformation is axisymmetric, so that all variables depend only on the radial coordinate r and the shear stress in the r-θ plane is zero throughout the arterial wall. Thus, the nontrivial equations of equilibrium on the deformed configuration are simplified as:

$$\frac{d\sigma_{rr}(r)}{dr}+\frac{\sigma_{rr}(r)-\sigma_{\theta\theta}(r)}{r}=0 \qquad (1)$$

$$\frac{d\sigma_{rz}(r)}{dr}+\frac{\sigma_{rz}(r)}{r}=0 \qquad (2)$$

where σ_{jk} (j, k = r, θ, z) denotes Cauchy stress. Using the approaches developed by Humphrey and Na (19) and Rachev *et al*. (32) while considering the boundary condition $\sigma_{rr}(r_i)=-P$ (P is blood pressure), the following expressions are obtained (see Appendix for details):

$$\sigma_{rr}(r) = \int_{r_i}^{r} \left(\lambda_\theta^2 \frac{\partial W}{\partial E_{\theta\theta}} - \lambda_r^2 \frac{\partial W}{\partial E_{rr}} \right) \frac{dr}{r} - P \tag{3}$$

$$\sigma_{\theta\theta}(r) = \sigma_{rr}(r) + \lambda_\theta^2 \frac{\partial W}{\partial E_{\theta\theta}} - \lambda_r^2 \frac{\partial W}{\partial E_{rr}} \tag{4}$$

$$\sigma_{zz}(r) = \sigma_{rr}(r) + \lambda_z^2 \frac{\partial W}{\partial E_{zz}} + (\xi_w^2 - \lambda_r^2) \frac{\partial W}{\partial E_{rr}} + 2\lambda_z \xi_w \frac{\partial W}{\partial E_{rz}} \tag{5}$$

where $W(E_{jk})$ is the strain energy, E_{jk} ($j, k = r, \theta, z$) is the Green strain (see Eq. *A4* in Appendix), λ_m ($m = r, \theta, z$) are stretch ratios, $\xi_w = dw/dR$ with w being the displacement that induces shear strain. It is noted that W is different for the arterial layers and hence two sets of parameters are needed for the intima and media-adventitia, respectively.

If we consider the boundary condition $\sigma_{rz}(r_i) = -\tau$ (τ is the blood shear stress at the inner surface, see Fig. 1*A*), the solution of *Eq. 2* can be obtained as $\sigma_{rz}(r) = -\tau r_i / r$, which implies that the perivascular tethering tissue must provide a shear force $-\tau r_i / r_o$ on the outer surface to balance the flow-induced shear load. The shear stress at given radial coordinate r can be used to compute ξ_w from *Eq. A11*:

$$\lambda_r \lambda_z \frac{\partial W}{\partial E_{rz}} + \lambda_r \xi_w \frac{\partial W}{\partial E_{rr}} = -\frac{\tau r_i}{r} \tag{6}$$

Fung's exponential strain energy function is used, which takes the following form (5,19):

$$W = \frac{C}{2}\{\exp[b_1 E_{\theta\theta}^2 + b_2 E_{zz}^2 + b_3 E_{rr}^2 + 2(b_4 E_{\theta\theta} E_{zz} + b_5 E_{zz} E_{rr} + b_6 E_{\theta\theta} E_{rr}) + b_7 (E_{rz}^2 + E_{zr}^2)] - 1\} \tag{7}$$

The constants C and b_1-b_7 are material parameters determined from experiment.

Simulation Parameters

The dimensions of the artery at zero-stress state were taken as R_i = 12.78 mm, R_o = 13.12 mm, Φ = 163° (unpublished data corresponding to Ref. 39). The intima (2~5 μm thick) was assumed to occupy 2% of the wall thickness (100~250 μm). The axial stretch ratio was chosen as λ_z = 1.4 (27). The Fung-model parameters C and b_1~b_7 in the intact porcine left anterior descending (LAD) artery are listed in Table 1 as previously reported by our group (39). The porcine coronary artery elastic modulus was estimated to be 170 kPa at physiological loading based on experimental data (26). According to Sato *et al*. (36), the Young's modulus of porcine aortic endothelial cells is on the order of 0.1 kPa. Hence the modulus in endothelium is approximately 1000 times smaller than the intact artery. Since complete model parameters are not available for intima, the parameter C was taken to be 1% and b_α (α = 1, …, 7) to be 10% of those of the intact porcine LAD artery reported by Wang *et al*. (39). To maintain the overall elastic stiffness of the artery at P = 100 mmHg, parameter C in the media-adventitia was increased by 1.65% from the value in intact wall (Table 1). Note that parameter C in Fung-model is a scale factor and parameter b_α reflects the material nonlinearity (curvature of stress-strain relation). Both C and b_α have been rescaled to make the elastic modulus (proportional to Cb_α) of intima 1000 times smaller. Sato *et al*. (36) considered a linear viscoelastic model for endothelial cells. Here we have chosen small b_α (Table 1) to ensure nearly linear stress-strain relationship of intima. More details about parameter selection are provided in Appendix.

The equations were solved numerically with finite difference method as outlined in Fig. 2. The solution was adopted when the difference between the radial stress at the outer surface ($\sigma_{rr}(r_o)$ in Eq. (3)) and the prescribed pressure boundary condition is less than 10^{-8} kPa. A simple test was done to verify that the unloaded state (P = 0, $\sigma_{rr}(r_o)$ = 0, and λ_z = 1.0) can be achieved with the above parameters (the resulting no-load r_i = 1.06 mm and r_o = 1.39 mm), for which the

residual stresses and strains are distributed across the arterial wall in a pattern similar to those shown in Ref. 5; e.g., circumferential components are compressive at the inner surface and tensile at the outer surface.

For the physiological state, we considered $\sigma_{rr}(r_i)$ = -13.33 kPa (the average value of systole and diastole pressure, P = 100 mmHg) while the constraint at the outer surface was taken to be $\sigma_{rr}(r_o)$ = -8.67 kPa (65 mmHg), which stems from the tethering myocardium (14). The choice of the external pressure was based on the consideration of myocardial constraint and the resulting outer radius of the vessel (1.81 mm at loaded state), consistent with the reported pressure-diameter relation of *in situ* porcine LAD artery (14).

RESULTS

Although only one numerical case is presented here, we found that similar results can be obtained in simulations with typical material properties. Hence, the present results have generality.

Under simultaneous internal pressure P = 100 mmHg, external pressure 65 mmHg, and blood shear stress τ = 1.5 Pa (15 dynes/cm^2), it is found that the shear strain is significant in the intima ($E_{rz} \approx$ -0.08) but close to zero in media-adventitia (Fig. 3*A*). The shear strain increases sharply at the interface of intima and media-adventitia (at normalized wall thickness of 2%, Fig. 3*C*), so does the radial strain (slightly) due to the contribution of ξ_w in E_{rr} (i.e., discontinuous of ξ_w results in discontinuous E_{rr}, *Eq. A4*). The radial stress is compressive in the whole vessel wall but the circumferential and axial stresses change abruptly from compressive to tensile across the interface of intima and media-adventitia layer (Fig. 3*B*). All normal stresses are nearly equal to the negative blood pressure (13.33 kPa) in the intima layer (Fig. 3*D*), indicating that the intima is

under a hydrostatic state approximately. The shear stress is always small, however, as expected (see right hand side of *Eq. 6*).

For comparison with the classic two-layer (intima-media and adventitia) model, we chose C = 5.11 kPa, b_1 = 2.47, b_2 = 3.09, b_3 = 0.95, b_4 = 0.45, b_5 = 0.06, b_6 = 0.10 for the intima-media layer and C = 9.05 kPa, b_1 = 0.62, b_2 = 2.27, b_3 = 1.67, b_4 = 0.34, b_5 = 0.11, b_6 = 0.07 for the adventitia layer (39). The b_7 = 2.89 was assumed for both layers and the intima-media was taken to be 60% of the total wall thickness. Under the same boundary conditions stated above, the (negative) maximum shear strain was found to be 3.8×10^{-5} at the inner surface of intima-media. Thus, the large flow-induced shear strain in intima is overshadowed in the intima-media and adventitia model.

For the same material properties in Table 1, the circumferential and axial strains do not change noticeably from Fig. 3*A* when the applied shear stress τ is increased to 9 Pa. However, the magnitude of shear strain in intima increases almost linearly with τ and it approaches the magnitude of normal strains, e.g., $|E_{rz}| \approx 0.4$ at τ = 9 Pa (Fig. 4*A*). The radial strain in media-adventitia is also similar to Fig. 3*A*, whereas its magnitude decreases nonlinearly with τ in intima (Fig. 4*A*) because the increase of term ξ_w^2 in *Eq. A4* leads to increasing E_{rr} (its magnitude decreases since E_{rr} is negative). This result implies that shear and radial strains in endothelial cells strongly depend on the flow conditions (normal flow vs. flow overload).

If the elastic stiffness in intima is smaller than the assumed value, the magnitude of shear strain will increase further and become comparable with the normal strains even under normal flow ($\tau \sim$ 1.5 Pa). Fig. 4*B* shows that the magnitude of shear strain on the inner surface increases (but radial strain decreases) nonlinearly with decreasing b_7 for intima (other parameters were

kept unchanged). At $b_7 = 0.05$, the magnitude of shear strain ($|E_{rz}| = 0.44$) approaches that of the circumferential and axial strains. The shear stress, on the other hand, remains several orders of magnitude smaller than the normal stresses even in flow-overload.

DISCUSSION

Our findings show that flow-induced shear strain in intima (largely composed of endothelium) may reach the magnitude of normal strains caused by blood pressure and axial stretch despite the relatively small shear load. This may have interesting implications as discussed below.

Strain or Stress as Mechanical Stimulus

Experiments by Lu and Kassab (25) revealed that the forward flow promotes Nitric Oxide (NO) production in arterial wall under normal flow but significantly reduces NO concentration under reversed flow. This phenomenon has been attributed to increased production of superoxide anion in reversed flow. The biological response of endothelial cells to the same magnitude of wall shear stress (but opposite in direction) is very different. It may be that the shear strain on the endothelial cells is very different depending on the direction as speculated below.

The residual strain in blood vessels is closely related to the remodeling process (10). There is enormous evidence that circumferential residual strain (characterized by the opening angle) in arteries changes with remodeling, e.g., Liu and Fung (24). Davies (7) pointed out that prolonged steady flow results in reorganization of endothelial surface and significant reduction of peak shear stress compared with no-flow conditions, which implies that a residual shear strain may exist in the arterial wall due to remodeling under chronic flow-induced shear. As illustrated in Fig. 5, if residual shear strain exists (left inset), the shear deformation might be quite different for the same shear stress under forward and reversed flows (middle inset and right inset). The

Final Accepted Manuscript: JAP-00199-2007.R2

flow-dependent reorientation of endothelial cells (7,30) could be related to the residual shear strain. Nonetheless, 3-D reconstructions of endothelial cells under various shear loadings are needed to confirm this hypothesis.

It has been well documented that stretch (or pressure) and shear (frictional flow force) are mechanical stimuli that influence the activity of endothelial and vascular smooth muscle cells (15,23). The flow reversal effect (25) supports the implication that strain may be the mechanical stimulus, because the biological response for the same shear stress (forward vs. reversed) is very different. It is also possible that the asymmetric response of endothelium to directionality may be due to different elastic properties in the forward and reverse directions. It is known that actin microfilaments (as well as other cytoskeletal elements) act very differently under tension and compression. This alternative hypothesis deserves further attention. In reality, both endothelial residual strain and differences in tension and compression of cytoskeletion may be implicated.

Rachev (33), Fridez *et al*. (8), Gleason and Humphrey (11) have studied the remodeling of carotid artery including passive and active behaviors by considering blood flow and pressure loading. The potential residual shear strain may be included in such analyses as it could play an important role in interpreting flow-related remodeling and mechanotransduction.

Critique of Method

Theoretically, if material property does not change along the axial direction, the arterial diameter will decrease along the flow direction. This is because flow is a result of pressure gradient. Using the Poiseuille's law (10), the internal shear stress can be approximated by

$$\tau = \frac{4\mu Q}{\pi r_i^3} = -\frac{r_i \Delta P}{2L} \qquad (8)$$

where μ denotes the coefficient of viscosity, Q is the rate of flow, and L equals the length along axis z when pressure drop is ΔP. Therefore, all the variables depend on coordinate z as well as on

r if flow exists. Nevertheless, this dependence on z can be viewed as a secondary effect in a typical blood vessel segment of interest (L ~ 1 cm), because the pressure drop is small and the change of lumen radius is insignificant. Thus our assumption that all variables are independent of z is reasonable.

Since the 3-D mechanical data for the endothelium do not exist, we assumed a Fung-type exponential energy function which is known to characterize many biological tissues (10) and estimated the respective material parameters. The 1-D modulus for the endothelium (36) was compared to that of vessel wall (39) and found to be 1000 times softer. The issue was to transform the 1-D experimental data reported for the endothelium to a 3-D constitutive relation. The material parameters selection for the estimated 3-D endothelial constitutive relation preserves both the linearity (determined by b_α) and the magnitude of the modulus (determined by Cb_α) obtained from the shear loading endothelial experiments. Although we selected the parameter C as 1% and b_α ($\alpha = 1, \ldots, 7$) as 10% of those of the intact artery, C of 10% and b_α of 1% would lead to the same conclusion. Similarly, other combinations of C and b_α lead to similar conclusion regarding the shear deformation as long as we maintain the observed linearity for the endothelium (decrease b_α) and modulus (Cb_α of 0.1%).

Here the media and adventitia have been regarded as one layer because their mechanical properties are on the same order. The conclusion that shear strain in intima may be significant will not change if media and adventitia layers are treated differently. We assumed that the intima is equal to 2% of the wall thickness, which is reasonable in young and healthy blood vessels. In diseased or aged arteries, the intima becomes thicker and stiffer (17), and its role becomes more important in tensile support (28,29). The thickened and hardened intima will change the strain distribution, which may affect mechanotransduction if strain is the stimulus for homeostasis.

Final Accepted Manuscript: JAP-00199-2007.R2

The arterial wall has been modeled as an elastic material and hence the stress and strain distributions are independent of the loading path. If the viscoelastic behavior of blood vessels is considered, the loading sequence must be taken into account. A 3-D finite element model for the viscoelastic deformation of endothelial cells has been considered in the literature (21) and is beyond the scope of the present study. Other issues such as mechanical property of perivascular tethering, non-Newtonian flow, complex geometry and heterogeneity of the vessel wall will make analytical modeling impractical. Some of these effects can be implemented in finite element method considering fluid-solid interaction, constraint of surrounding tissues, etc. (20,41).

It should be noted that our modeling has been conducted on the macroscopic level based on continuum mechanics. Therefore, stress and strain in the arterial wall must be interpreted as the average values of various microstructural constituents. This is different from the works of Huang *et al*. (18) and Karcher *et al*. (21) as well as other investigations where details of stresses and strains in the individual cells with realistic shapes and geometries have been considered. Despite the lack of microstructural details, the present model captures the essence of the question raised.

Chaudhry *et al*. (3) reported that residual stress and strain reduce the circumferential stress gradient in oscillating arterial wall. Cinthio *et al*. (6) studied the longitudinal movement of arterial wall in cardiac cycle and concluded that the shear strain in artery may be substantial. Based on a general formulation including dynamics and smooth muscle active terms developed by Humphrey and Na (19), the current model can be extended to investigate arterial behavior involving pulsatile blood flow, smooth muscle cell activity, and other physiological features.

Summary and Significance of Study

A computational model that takes into account coupled pressure and shear loading was used to analyze stress and strain distributions in the porcine coronary artery. It is found that the flow-induced shear strain in intima can be as large as normal strains caused by internal blood pressure. This finding may have significant implications for interpreting vascular behaviors such as vasoactivity due to change of blood pressure and flow, arterial wall remodeling and pathophysiology (atherosclerosis). It may shed light on the mechanical stimulation mechanisms in the endothelial cell.

It is suggested that the intima layer should be considered separately to investigate the role of flow-induced shear, since the deformation in the intima may be overshadowed by the media and adventitia layers which have much larger elastic moduli (flow-induced shear strain was found to be $E_{rz} \approx -3\times10^{-5}$ in a one-layer model with intact properties listed in Table 1 or a classic intima-media and adventitia two-layer model as mentioned earlier). From the numerical results of the intima and media-adventitia two-layer model, we hypothesize that shear strain may be a stimulus for the endothelium. In this regard, strain may be a good measure to correlate with biochemical response of blood vessels. This hypothesis needs to be explored in future experimental studies.

Final Accepted Manuscript: JAP-00199-2007.R2

APPENDIX

Deformation and Stress

As illustrated in Fig. 1, the coordinates in the deformed configuration (r, θ, z) are related to those in the zero-stress state (R, Θ, Z) by

$$r = r(R), \quad \theta = \chi\Theta, \quad z = \lambda_z Z + w(R) \tag{A1}$$

where $\chi = \pi/(\pi - \Phi)$, λ_z is the stretch ratio in axial direction, w is the relative displacement in z direction. The deformation gradient matrix with respect to the zero-stress state is

$$[F_{jk}] = \begin{bmatrix} \frac{\partial r}{\partial R} & \frac{\partial r}{R\partial\Theta} & \frac{\partial r}{\partial Z} \\ \frac{r\partial\theta}{\partial R} & \frac{r\partial\theta}{R\partial\Theta} & \frac{r\partial\theta}{\partial Z} \\ \frac{\partial z}{\partial R} & \frac{\partial z}{R\partial\Theta} & \frac{\partial z}{\partial Z} \end{bmatrix} = \begin{bmatrix} \lambda_r & 0 & 0 \\ 0 & \lambda_\theta & 0 \\ \xi_w & 0 & \lambda_z \end{bmatrix} \tag{A2}$$

where $j, k = r, \theta, z$ and

$$\lambda_r = \frac{dr}{dR}, \quad \lambda_\theta = \frac{\chi r}{R}, \quad \xi_w = \frac{dw}{dR} \tag{A3}$$

The corresponding Green strain tensor $E_{jk} = \frac{1}{2}(F_{lj}F_{lk} - \delta_{jk})$ is

$$[E_{jk}] = \frac{1}{2}\begin{bmatrix} \lambda_r^2 + \xi_w^2 - 1 & 0 & \lambda_z\xi_w \\ 0 & \lambda_\theta^2 - 1 & 0 \\ \lambda_z\xi_w & 0 & \lambda_z^2 - 1 \end{bmatrix} \tag{A4}$$

If we assume incompressibility ($\det[F_{jk}] = 1$ in *Eq. A2*), we have

$$\lambda_r = \frac{R}{\chi\lambda_z r} \tag{A5}$$

and

$$r = \sqrt{r_i^2 + \frac{R^2 - R_i^2}{\chi\lambda_z}} \tag{A6}$$

Cauchy stress tensor is computed as (19)

$$\sigma_{jk} = F_{jl}F_{km}\frac{\partial W}{\partial E_{lm}} + H\delta_{jk} \qquad (A7)$$

where $H = H(r)$ is the hydrostatic stress due to incompressibility. Specially, the nonzero stress components are

$$\sigma_{rr} = \lambda_r^2\frac{\partial W}{\partial E_{rr}} + H \qquad (A8)$$

$$\sigma_{\theta\theta} = \lambda_\theta^2\frac{\partial W}{\partial E_{\theta\theta}} + H \qquad (A9)$$

$$\sigma_{zz} = \lambda_z^2\frac{\partial W}{\partial E_{zz}} + \xi_w^2\frac{\partial W}{\partial E_{rr}} + 2\lambda_z\xi_w\frac{\partial W}{\partial E_{rz}} + H \qquad (A10)$$

$$\sigma_{rz} = \lambda_r\lambda_z\frac{\partial W}{\partial E_{rz}} + \lambda_r\xi_w\frac{\partial W}{\partial E_{rr}} \qquad (A11)$$

Equations *3-6* can be derived from *Eqs. 1*, *2*, and *A8-A11* when considering boundary conditions in the radial direction.

Material Parameters for Fung Model

The parameters in the normal directions for an intact vessel were taken as the average values reported by Wang *et al.* (39). For the parameter b_7, we assumed that the shear modulus in the *rz* plane is similar to that in the θz plane. The shear modulus 160 kPa in the θz plane (27) for λ_z = 1.4 and circumferential stress 90 kPa ($\lambda_\theta \approx 1.6$) were used to estimate b_7 = 2.89 for Fung model.

The mechanical behavior of endothelium, which is significantly different when the cells are viewed as fluid-like or solid-like (9), is essential to predict the correct stress and strain in intima. Caille *et al.* (2) adopted an isotropic material model (Mooney–Rivlin law) to fit the experimental force-deformation curves of bovine aortic endothelial cells and determined that their elastic moduli are on the order of 0.5 kPa for spread and round cells and 5.0 kPa for cells

with nuclei. Sato *et al*. (36) reported the linear viscoelastic properties of cultured endothelial cells under shear stress. They estimated that the Young's modulus of porcine aortic endothelial cells is on the order of 0.1 kPa. Considering that the porcine coronary artery elastic modulus is about 170 kPa (26), it is rationalized that the elastic stiffness of porcine endothelium is approximately 1000 times smaller than that of the overall vessel. Due to the lack of data, we assumed that Fung model applies to the intima layer. The properties for intima (basal lamina and subendothelial layer are assumed to have the same property as endothelium) as given in Table 1 were selected to ensure this modulus criterion (modulus is proportional to the product of C and b_α).

It should be noted that shear modulus in the rz plane may be different from that in the θz plane. In quantitative modeling, accurate experimental results are desired. Since the endothelial cells are soft and thin, it is difficult to obtain their 3-D constitutive equation and material parameters. Hence, direct measurement of stress-strain relationship of intima remains a technical challenge.

ACKNOWLEDGEMENTS

W.Z. thanks Dr. Xiao Lu and Chong Wang for helpful discussions. This research was supported in part by the National Institute of Health-National Heart, Lung, and Blood Institute Grant 2 R01 HL055554-11.

REFERENCES

1. **Barakat AI, Lieu DK, and Gojova A.** Secrets of the code: do vascular endothelial cells use ion channels to decipher complex flow signals? *Biomaterials* 27: 671-678, 2006.
2. **Caille N, Thoumine O, Tardy Y, and Meister JJ.** Contribution of the nucleus to the mechanical properties of endothelial cells. *J Biomech* 35: 177-187, 2002.
3. **Chaudhry HR, Bukiet B, Davis A, Ritter AB, and Findley T.** Residual stresses in oscillating thoracic arteries reduce circumferential stresses and stress gradients. *J Biomech* 30: 57-62, 1997.
4. **Chien S, Li S, and Shyy JYJ.** Effects of mechanical forces on signal transduction and gene expression in endothelial cells. *Hypertension* 31: 162-169, 1998.
5. **Chuong CJ and Fung YC.** On residual stresses in arteries. *J Biomech Eng* 108: 189-192, 1986.
6. **Cinthio M, Ahlgren AR, Bergkvist J, Jansson T, Persson HW, and Lindstrom K.** Longitudinal movements and resulting shear strain of the arterial wall. *Am J Physiol Heart Circ Physiol* 291: H394-H402, 2006.
7. **Davies PF.** Flow-mediated endothelial mechanotransduction. *Physiol Rev* 75: 519-560, 1995.
8. **Fridez P, Rachev A, Meister JJ, Hayashi K, and Stergiopulos N.** Model of geometrical and smooth muscle tone adaptation of carotid artery subject to step change in pressure. *Am J Physiol Heart Circ Physiol* 280: H2752-H2760, 2001.
9. **Fung YC and Liu SQ.** Elementary mechanics of the endothelium of blood-vessels. *J Biomech Eng* 115: 1-12, 1993.
10. **Fung YC.** *Biomechanics: Circulation*, 2nd Ed. New York: Springer, 1997.

11. **Gleason RL and Humphrey JD.** A 2D constrained mixture model for arterial adaptations to large changes in flow, pressure and axial stretch. *Math Med Biol* 22: 347-369, 2005.

12. **Guo XM and Kassab GS.** Distribution of stress and strain along the porcine aorta and coronary arterial tree. *Am J Physiol Heart Circ Physiol* 286: H2361-H2368, 2004.

13. **Guo XM, Lu X, and Kassab GS.** Transmural strain distribution in the blood vessel wall. *Am J Physiol Heart Circ Physiol* 288: H881-H886, 2005.

14. **Hamza LH, Dang Q, Lu X, Mian A, Molloi S, and Kassab GS.** Effect of passive myocardium on the compliance of porcine coronary arteries. *Am J Physiol Heart Circ Physiol* 285: H653-H660, 2003.

15. **Harrison DG, Widder J, Grumbach I, Chen W, Weber M, and Searles C.** Endothelial mechanotransduction, nitric oxide and vascular inflammation. *J Intern Med* 259: 351-363, 2006.

16. **Holzapfel GA, Gasser TC, and Ogden RW.** A new constitutive framework for arterial wall mechanics and a comparative study of material models. *J Elasticity* 61: 1-48, 2000.

17. **Holzapfel GA, Sommer G, Gasser CT, and Regitnig P.** Determination of layer-specific mechanical properties of human coronary arteries with nonatherosclerotic intimal thickening and related constitutive modeling. *Am J Physiol Heart Circ Physiol* 289: H2048-H2058, 2005.

18. **Huang YQ, Rumschitzki D, Chien S, and Weinbaum S.** A fiber matrix model for the filtration through fenestral pores in a compressible arterial intima. *Am J Physiol Heart Circ Physiol* 272: H2023-H2039, 1997.

19. **Humphrey JD and Na S.** Elastodynamics and arterial wall stress. *Ann Biomed Eng* 30: 509-523, 2002.

20. **Hunter KS, Lanning CJ, Chen SYJ, Zhang YH, Garg R, Ivy DD, and Shandas R.** Simulations of congenital septal defect closure and reactivity testing in patient-specific models of the pediatric pulmonary vasculature: a 3D numerical study with fluid-structure interaction. *J Biomech Eng* 128: 564-572, 2006.

21. **Karcher H, Lammerding J, Huang HD, Lee RT, Kamm RD, and Kaazempur-Mofrad MR.** A three-dimensional viscoelastic model for cell deformation with experimental verification. *Biophys J* 85: 3336-3349, 2003.

22. **Kassab GS and Navia JA.** Biomechanical considerations in the design of graft: the homeostasis hypothesis. *Annu Rev Biomed Eng* 8: 499-535, 2006.

23. **Lehoux S.** Redox signalling in vascular responses to shear and stretch. *Cardiovasc Res* 71: 269-279, 2006.

24. **Liu SQ and Fung YC.** Relationship between hypertension, hypertrophy, and opening angle of zero-stress state of arteries following aortic constriction. *J Biomech Eng* 111: 325-335, 1989.

25. **Lu X and Kassab GS.** Nitric oxide is significantly reduced in ex vivo porcine arteries during reverse flow because of increased superoxide production. *J Physiol* 561: 575-582, 2004.

26. **Lu X, Pandit A, and Kassab GS.** Biaxial incremental homeostatic elastic moduli of coronary artery: two-layer model. *Am J Physiol Heart Circ Physiol* 287: H1663-H1669, 2004.

27. **Lu X, Yang J, Zhao JB, Gregersen H, and Kassab GS.** Shear modulus of porcine coronary artery: contributions of media and adventitia. *Am J Physiol Heart Circ Physiol* 285: H1966-H1975, 2003.

28. **Masawa N, Glagov S, and Zarins CK.** Quantitative morphologic study of intimal thickening at the human carotid bifurcation .1. axial and circumferential distribution of maximum intimal thickening in asymptomatic, uncomplicated plaques. *Atherosclerosis* 107: 137-146, 1994.

29. **Masawa N, Glagov S, and Zarins CK.** Quantitative morphologic study of intimal thickening at the human carotid bifurcation .2. the compensatory enlargement response and the role of the intima in tensile support. *Atherosclerosis* 107: 147-155, 1994.

30. **Michiels C.** Endothelial cell functions. *J Cell Physiol* 196: 430-443, 2003.

31. **Pyke KE and Tschakovsky ME.** The relationship between shear stress and flow-mediated dilatation: implications for the assessment of endothelial function. *J Physiol* 568: 357-369, 2005.

32. **Rachev A, Stergiopulos N, and Meister JJ.** Theoretical study of dynamics of arterial wall remodeling in response to changes in blood pressure. *J Biomech* 29: 635-642, 1996.

33. **Rachev A.** A model of arterial adaptation to alterations in blood flow. *J Elasticity* 61: 83-111, 2000.

34. **Rachev A.** Theoretical study of the effect of stress-dependent remodeling on arterial geometry under hypertensive conditions. *J Biomech* 30: 819-827, 1997.

35. **Resnick N, Yahav H, Shay-Salit A, Shushy M, Schubert S, Zilberman LCM, and Wofovitz E.** Fluid shear stress and the vascular endothelium: for better and for worse. *Prog Biophys Mol Biol* 81: 177-199, 2003.

36. **Sato M, Ohshima N, and Nerem RM.** Viscoelastic properties of cultured porcine aortic endothelial cells exposed to shear stress. *J Biomech* 29: 461-467, 1996.

37. **Takamizawa K and Hayashi K.** Strain-energy density-function and uniform strain hypothesis for arterial mechanics. *J Biomech* 20: 7-17, 1987.

38. **Tarbell JM, Weinbaum S, and Kamm RD**. Cellular fluid mechanics and mechanotransduction. *Ann Biomed Eng* 33: 1719-1723, 2005.

39. **Wang C, Garcia M, Lu X, Lanir Y, and Kassab GS.** Three-dimensional mechanical properties of porcine coronary arteries: a validated two-layer model. *Am J Physiol Heart Circ Physiol* 291: H1200-H1209, 2006.

40. **Weinbaum S, Zhang XB, Han YF, Vink H, and Cowin SC**. Mechanotransduction and flow across the endothelial glycocalyx. *Proc Natl Acad Sci USA* 100: 7988-7995, 2003.

41. **Zhang W, Herrera C, Atluri SN, and Kassab GS.** Effect of surrounding tissue on vessel fluid and solid mechanics. *J Biomech Eng* 126: 760-769, 2004.

42. **Zhang W, Herrera C, Atluri SN, and Kassab GS.** The effect of longitudinal pre-stretch and radial constraint on the stress distribution in the vessel wall: a new hypothesis. *Mech Chem Biosyst* 2: 41-52, 2005.

Final Accepted Manuscript: JAP-00199-2007.R2

Table 1

Fung-model material properties for porcine left anterior descending coronary artery

	C (kPa)	b_1	b_2	b_3	b_4	b_5	b_6	b_7
intact artery	8.76	1.21	3.39	0.79	0.35	0.11	0.10	2.89
intima	0.0876	0.121	0.339	0.079	0.035	0.011	0.010	0.289
media-adventitia	8.90	1.21	3.39	0.79	0.35	0.11	0.10	2.89

Final Accepted Manuscript: JAP-00199-2007.R2

FIGURE LEGENDS

Figure 1. A schematic representation of an artery under internal pressure and shear (*A*), the zero-stress sate (*B*), the deformed cross section (*C*), and the two-layer model (*D*). R_i and R_o, r_i and r_o, are the inner and outer radii in the (R, Θ, Z) and (r, θ, z) coordinate systems, respectively. Note that under flow-induced shear loading, the material points initially in the same Z-plane do not remain in a plane (they follow Lagrange coordinates).

Figure 2. Flow chart of the numerical method. $N = 26$ (two nodes are defined at the interface).

Figure 3. Green strain (*A*) and Cauchy stress (*B*) distributions across the vessel wall thickness (P = 100 mmHg, τ = 1.5 Pa). (*C*) and (*D*) are magnifications near the inner surface.

Figure 4. Variations of shear strain and radial strain magnitudes on the inner arterial wall when applied shear stress τ is increased (*A*) and parameter b_7 in intima is decreased (*B*).

Figure 5. Schematic drawing of the arterial wall at zero-stress state with a released residual shear strain (left), under normal flow (middle), and reverse flow (right). The horizontal arrows indicate the shear stress directions.

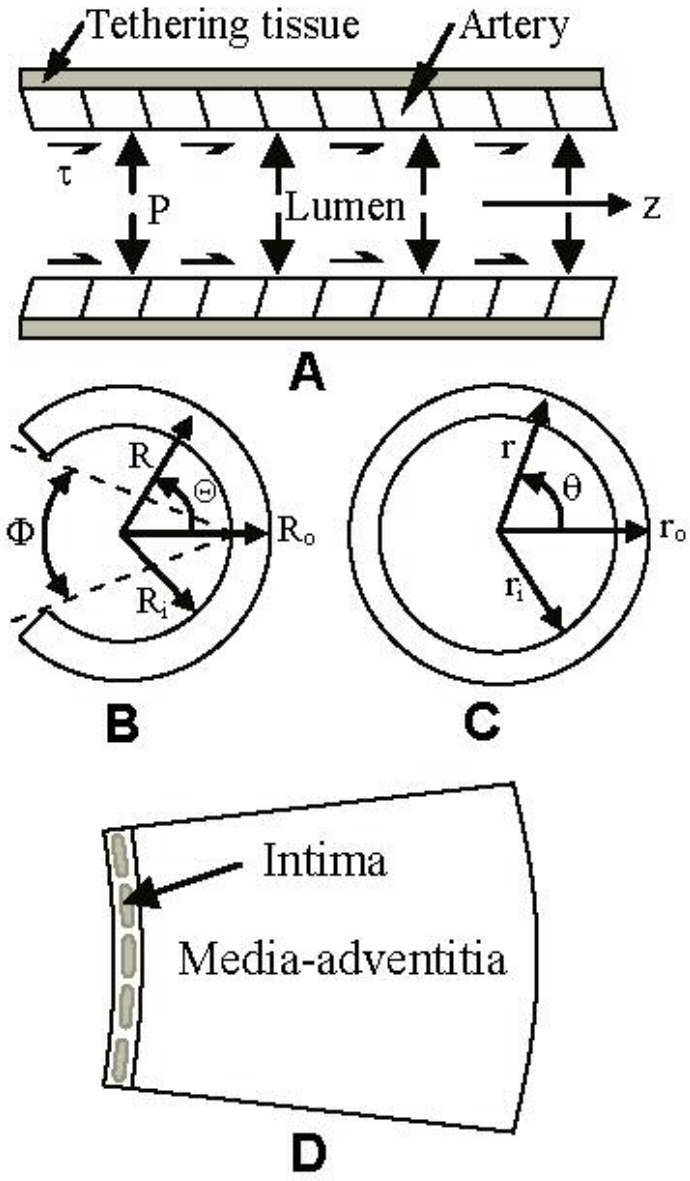

47x78mm (200 x 200 DPI)

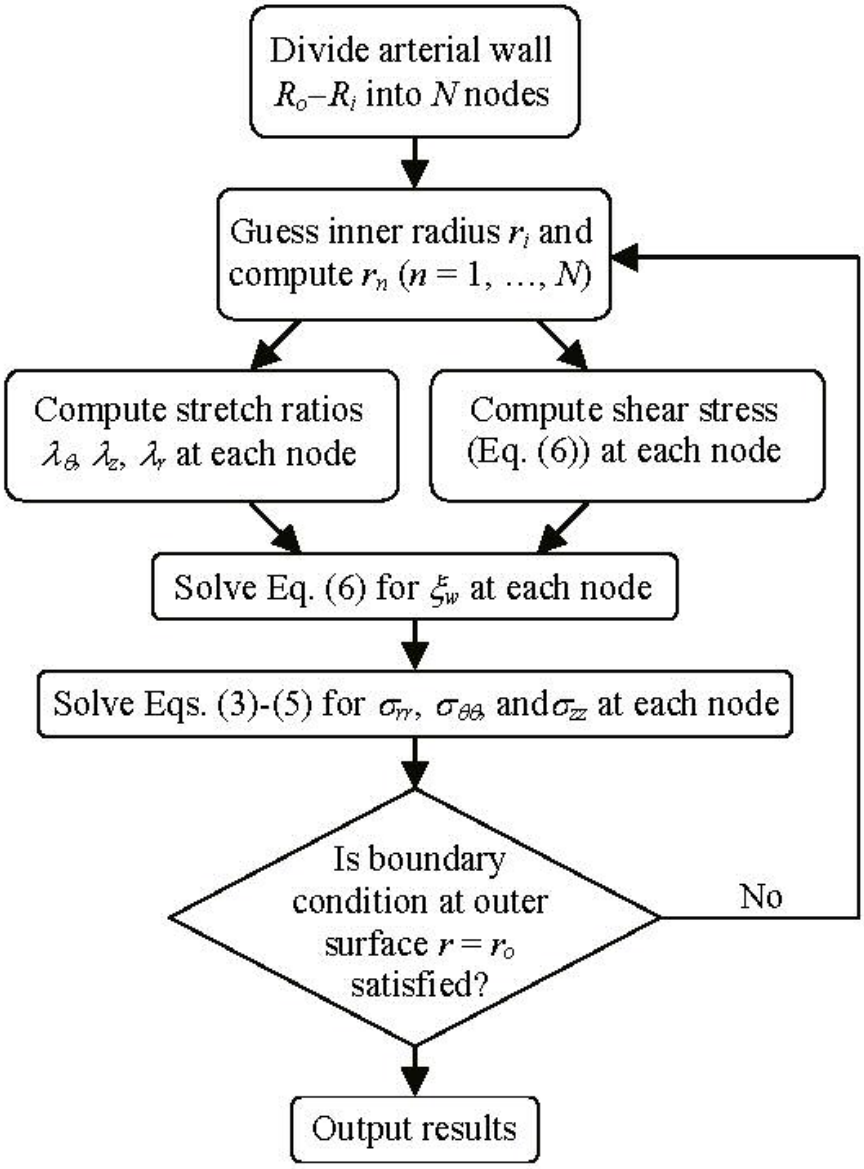

73x93mm (200 x 200 DPI)

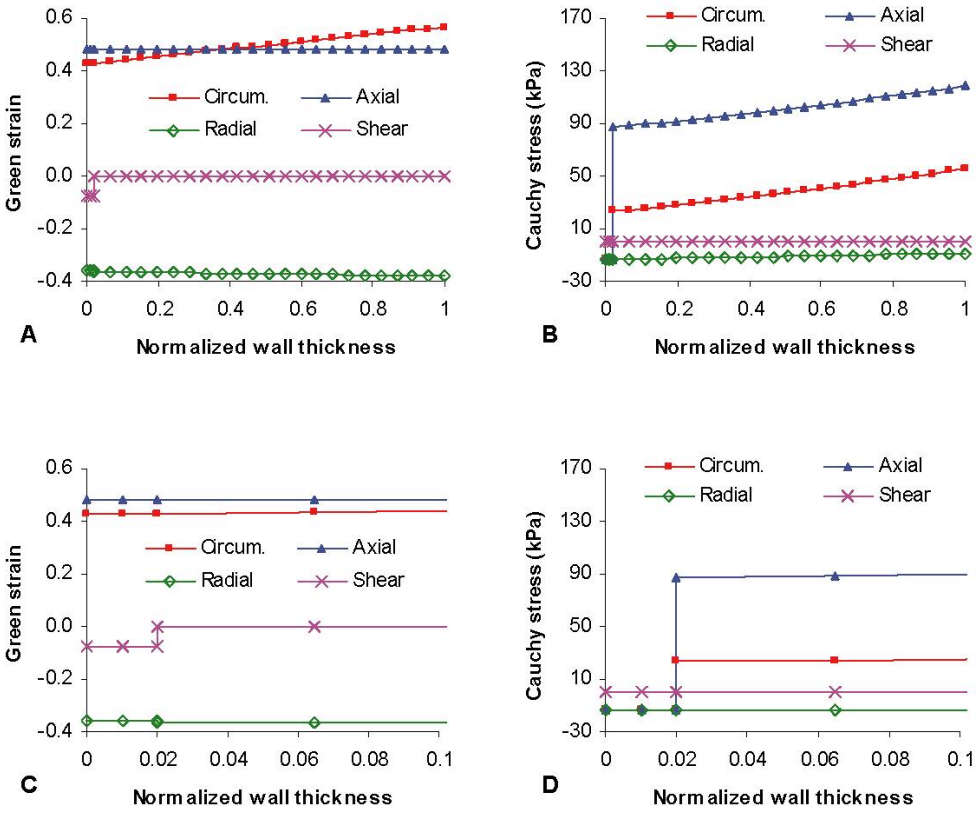

146x120mm (200 x 200 DPI)

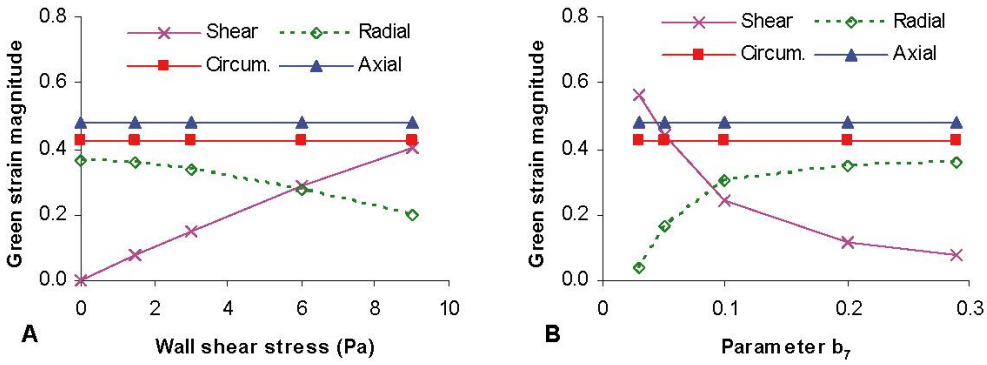

146x54mm (200 x 200 DPI)

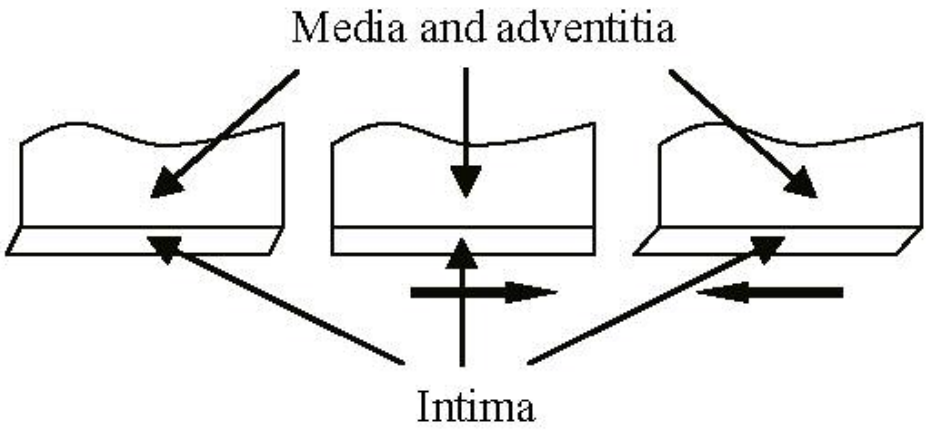

69x35mm (200 x 200 DPI)